Direct Dynamics Calculation for the Double Proton Transfer in Formic Acid Dimer

Yongho Kim

Contribution from the Department of Chemistry, Kyung Hee University, Yongin-Kun, Kyunggi-Do, 449-701 Korea

Received September 15, 1995[⊗]

Abstract: The dynamics of the double proton transfer in formic acid dimer (FAD) complex has been studied by the direct dynamics approach with variational transition state theory using multidimensional semiclassical tunneling approximations. High-level *ab initio* quantum mechanical calculations were performed to estimate the energetics of the double proton transfer. Dimerization energies and the barrier height have been calculated at the G2* level of theory, which yields −14.2 and 8.94 kcal mol^{-1}, respectively. A quantum mechanical potential energy surface has been constructed using the AM1 Hamiltonian with specific reaction parameters (AM1-SRP) which are obtained by adjusting the standard AM1 parameters to reproduce the energetics by high-level *ab initio* quantum mechanical calculation. The minimum energy path has been calculated on this potential energy surface and other characteristics of the surface were calculated as needed. The two protons are transferred synchronously, so the transition state possesses D_{2h} symmetry. The reaction path curvature is very large, so the tunneling coefficient is also very large as calculated by the large-curvature ground-state tunneling approximation (LCG3). The distance which the proton hops during tunneling is about 0.429 Å. This is a very long distance compared with the normal single proton transfer. Before the tunneling the hydrogenic motion is minimal. Mostly the heavy atoms move to bring the two formic acid molecules closer. The kinetic isotope effect (KIE) was also calculated. The tunneling contribution to the KIE is not extremely large since not only two protons but two deuterium atoms tunnel well. The quasiclassical contribution to the KIE is quite large due to the synchronous motion of the two protons.

Introduction

Proton transfer is one of the simplest and the most fundamental reactions in chemistry. It is important in oxidation−reduction reactions in many chemical and biological reactions, so it has been studied extensively.[1,2] However, most of the studies of proton transfer have been done for a single proton transfer, in which one proton is transferred during the reaction. Multiproton transfers in which more than one proton is transferred, either synchronously or asynchronously, have not been extensively studied. There is, particularly, little theoretical work on dynamics of such systems. Examples of multiproton transfer are proton relay systems in enzymes, certain proton transfers in hydrogen-bonded water complexes, and proton transfers in prototropic tautomerisms. Recently Limbach *et al*. have studied double proton transfer in prototropic tautomerisms for many formamidine systems and porphyrins using the dynamic NMR technique.[3−6] They reported rates and the kinetic isotope effects for both concerted[6,7] and stepwise[3−5] double proton transfer. Ernst *et al*. have studied the double proton transfer in the crystalline benzoic acid dimer and measured the kinetic isotope effects.[8,9] They have suggested the predominant tunneling effect on the double proton transfer even at room temperature. Hobza *et al*. have studied the potential energy surface (PES) for double proton transfer in the adenine−tymine base pair using various computational methods.[10−12] They have reported that the character of the PES such as the barrier for the double proton transfer strongly depends on the theoretical level of calculation: the size of the basis set and the inclusion of correlation energy.[12]

Formic acid dimer (FAD) is one of most extensively studied systems both experimentally and theoretically since it forms strong hydrogen bonds, so it is fairly easy to measure the IR and Raman frequencies.[13−15] It is also one of the simplest examples of a multiproton transfer system in which the constituents are held together by two hydrogen bonds, so it can be used as a model of many chemically and biologically important multiproton transfers. Most of the earlier studies have focused on the geometrical change on dimerization, and the energetic stabilization due to the hydrogen bonds in the dimer.[16−18] Recently many theoretical studies with *ab initio* quantum chemical methods at various levels have been carried out to predict the structures of the dimer and the potential energy surface for the various double proton transfer processes.[19−24] Scheiner *et al*. have studied and reviewed the potential energy surface for the proton transfer and the dimerization energy in a hydrogen-bonded system.[25,26]

[⊗] Abstract published in *Advance ACS Abstracts,* February 1, 1996.

(1) Bender, M. L. *Mechanisms of Homogeneous Catalysis from Protons to Proteins*; John Wiley & Sons: New York, 1971; Chapters 2, 4, and 5.
(2) Melander, L.; Saunders, W. H. J. *Reaction Rates of Isotopic Molecules*; John Wiley and Sons: New York, 1980; p 152.
(3) Schlabach, M.; Limbach, H.-H.; Bunnenberg, E.; Shu, A. Y. L.; Tolf, B.-R.; Djerassi, C. *J. Am. Chem. Soc.* **1993**, *115*, 4554.
(4) Scherer, G.; Limbach, H.-H. *J. Am. Chem. Soc.* **1994**, *116*, 1230.
(5) Scherer, G.; Limbach, H.-H. *J. Am. Chem. Soc.* **1989**, *111*, 5946.
(6) Meschede, L.; Limbach, H.-H. *J. Phys. Chem.* **1991**, *95*, 10267.
(7) Gerritzen, D.; Limbach, H.-H. *J. Am. Chem. Soc.* **1984**, *106*, 869.
(8) Meyer, R.; Ernst, R. R. *J. Chem. Phys.* **1990**, *93*, 5518.
(9) Stöckli, A.; Meier, B. H.; Kreis, R.; Meyer, R.; Ernst, R. R. *J. Chem. Phys.* **1990**, *93*, 1502.
(10) Florián, J.; Hrouda, V.; Hobza, P. *J. Am. Chem. Soc.* **1994**, *116*, 1457.
(11) Hrouda, V.; Florián, J.; Hobza, P. *J. Phys. Chem.* **1993**, *97*, 1542.
(12) Hrouda, V.; Florián, J.; Polásek, M.; Hobza, P. *J. Phys. Chem.* **1994**, *98*, 4742.
(13) Bertie, J. E.; Michaelian, K. H.; Eysel, H. H. *J. Chem. Phys.* **1986**, *85*, 4779.
(14) Bertie, J. E.; Michaelian, K. H. *J. Chem. Phys.* **1982**, *76*, 886.
(15) Millikan, R. C.; Pitzer, K. S. *J. Am. Chem. Soc.* **1958**, *80*, 3515.
(16) Lazaar, K. I.; Bauer, S. H. *J. Am. Chem. Soc.* **1985**, *107*, 3769.
(17) Almenningen, A.; Bastiansen, O.; Motzfeldt, T. *Acta. Chem. Scand.* **1970**, *24*, 747.
(18) Karpfen, A. *Chem. Phys.* **1984**, *88*, 415.
(19) Agranat, I.; Riggs, N. V.; Radom, L. *J. Chem. Soc., Chem. Commun.* **1991**, 80.
(20) Svensson, P.; Bergman, N.-Å.; Ahlberg, P. *J. Chem. Soc., Chem. Commun.* **1990**, 82.

0002-7863/96/1518-1522$12.00/0 © 1996 American Chemical Society

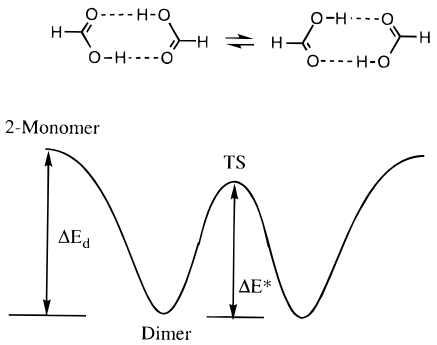

Figure 1. Schematic potential energy diagram for the double proton transfer between formic acid dimer.

Most studies of the double proton transfer have been based on a one-dimensional double well potential.[27,28] Therefore the detailed dynamic features of the double proton transfer in FAD, such as tunneling and the effect of isotopic substitution, are not very well understood yet. In 1987, Chang *et al*.[29] reported a reaction path Hamiltonian calculation of the tunneling splitting for FAD which yielded 0.3 cm^{-1}. Later, in 1991, Shida *et al*.[30] calculated the tunneling splitting of 0.004 cm^{-1} by the same method but with a better potential energy surface. The effective barrier height including zero-point energy was 11.8 kcal mol^{-1}, and the most probable path crossed the barrier more than 6 kcal mol^{-1} below the top. They showed that the effective tunneling path was very different from the minimum energy path (MEP) for the double proton transfer in FAD.[30] The behavior that they observed is consistent with the expected reaction dynamics for the heavy−light−heavy mass combinations, such as the proton transfer between two oxygens.[31,32]

Figure 1 shows a schematic one-dimensional potential energy diagram for the double proton transfer. A single transition state structure with D_{2h} symmetry is obtained in many calculations, which suggests that the double proton transfer in the FAD has a single transition state and proceeds through a concerted mechanism. The dimerization energies, ΔE_d, and the potential energy barrier, ΔE^*, have been calculated using many different levels of quantum mechanical theory.[33] The values of ΔE_d and ΔE^* vary significantly with the level of the quantum mechanical calculations. The correlation effect seems very important to these energies.[33] In the present study, the G2* level of quantum mechanical calculation has been used to estimate ΔE_d and ΔE^*. In G2* theory, polarization functions on hydrogen were added to the standard G2 level basis sets.[34−36] The semiempirical molecular orbital method at the NDDO level, such as used in the AM1 or PM3 general parametrizations, was used with specific reaction parameters (SRP) to calculate the minimum energy path and the potential energy along it.[37] The standard NDDO parameters were adjusted to reproduce the experimental dimerization energy and the theoretical potential energy barrier height determined by the G2* level calculations.[32,37] Direct dynamics calculations have been carried out for the double proton transfer by variational transition state theory including tunneling contribution by multidimensional semiclassical approximations. The AM1 Hamiltonian was used as a starting point for the SRP adjustments, since it reproduces the dimerization energy and the structure of FAD better than the PM3. However the AM1 method produced an unreasonably large barrier height for the double proton transfer. So the standard AM1 parameters were modified to reproduce the values of ΔE_d and ΔE^* from experiment and G2* calculations, respectively, and the geometries of the monomer, dimer, and the transition state. The modified parameters, called AM1-SRP, were used for the direct dynamic calculations.

Theory

Rate constants were calculated by the variational transition state theory.[31,38−43] The transition state was located at the position on the minimum energy path (MEP) where the calculated rate is a minimum. The Born−Oppenheimer potential of the MEP is called $V_{MEP}(s)$, where s is the reaction coordinate parameter, and the canonical variational transition state theory rate constant is given by[31,44]

$$k^{CVT}(T) = \min_s k^{GT}(T,s) = \sigma\frac{\tilde{k}T}{h}\frac{Q^{GT}(T,s_*^{CVT})}{Q^R}\exp[-V_{MEP}(s_*^{CVT})] \quad (1)$$

The superscript GT denotes the generalized transition state theory; $\tilde{k}$ is the Boltzman constant; h is Plank's constant: s_*^{CVT} is the value of s at which k^{GT} is minimized, that is, the location of the canonical variational transition state; σ is the symmetry factor; and Q^{GT} and G^R are partition functions for the generalized transition state and reactants, respectively.

In order to include the tunneling effect, the calculated rate constant, $k^{CVT}(T)$, is multiplied by a transmission coefficient, $\kappa^{CVT/G}$.

$$k^{CVT/G}(T) = \kappa^{CVT/G}(T)\, k^{CVT}(T) \quad (2)$$

The transmission coefficient is defined as the ratio of the thermally averaged quantal transmission probability, $P^G(E)$, to the thermally averaged classical transmission probability, $P_C^{CVT/G}(E)$.

$$\kappa^{CVT/G}(T) = \frac{\int_0^\infty P^G(E)e^{-E/\tilde{k}T}\,dE}{\int_0^\infty P_C^{CVT/G}(E)e^{-E/\tilde{k}T}\,dE} \quad (3)$$

The value of $P_C^{CVT/G}(E)$ is unity above the classical threshold energy and is zero below. Several semiclassical tunneling approximations were

(21) Tachibana, A.; Koizumi, M.; Tanaka, E.; Yamabe, T.; Fukui, K. *J. Mol. Struct.* **1989**, *200*, 207.
(22) Tachibana, A.; Ishizuka, N.; Yamaba, T. *J. Mol. Struct.* **1991**, *228*, 259.
(23) Topaler, M. S.; Mamaev, V. M.; Gluz, Y. B.; Minkin, V. I.; Simkin, B. Y. *J. Mol. Struct.* **1991**, *236*, 393.
(24) Zielinski, T. J.; Poirier, R. A. *J. Comput. Chem.* **1984**, *5*, 466.
(25) Scheiner, S. In *Reviews in Computational Chemistry*; Lipkowitz, K. B., Boyd, D. B., Eds.; VCH: New York, 1991; Vol. 2, p 165.
(26) Scheiner, S. In *Proton Transfer in Hydrogen Bonded Systems*; Bountis, T., Ed.; NATO ASI Series B291; Plenum: New York, 1992; p 29.
(27) Graf, F.; Meyer, R.; Ha, T.-K.; Ernst, R. R. *J. Chem. Phys.* **1981**, *75*, 2914.
(28) Hayashi, S.; Umemura, J.; Kato, S.; Morokuma, K. *J. Phys. Chem.* **1984**, *88*, 1330.
(29) Chang, Y.-T.; Yamaguchi, Y.; Miller, W. H.; Schefer, H. F., III *J. Am. Chem. Soc.* **1987**, *109*, 7245.
(30) Shida, N.; Barbara, P. F.; Almlof, J. *J. Chem. Phys.* **1991**, *94*, 3633.
(31) Truhlar, D. G.; Isaacson, A. D.; Garrett, B. C. In *Theory of Chemical Reaction Dynamics*; Baer, M., Ed.; CRC Press: Boca Raton, FL, 1985; Vol. 4, p 65.
(32) Liu, Y.-P.; Lu, D.-h.; Gonzalez-Lafont, A.; Truhlar, D. G.; Garrett, B. C. *J. Am. Chem. Soc.* **1993**, *115*, 7806.
(33) Svensson, P.; Bergman, N.-Å.; Ahlberg, P. *J. Chem. Soc., Chem. Commun.* **1990**, 862.
(34) Pople, J. A.; Head-Gordon, M.; Fox, D. J.; Raghavachari, K.; Curtis, L. A. *J. Chem. Phys.* **1989**, *90*, 5652.
(35) Curtiss, L. A.; Raghavachari, K.; Trucks, G. W.; Pople, J. A. *J. Chem. Phys.* **1991**, *94*, 7221.
(36) Curtiss, L. A.; Jones, C.; Trucks, G. W.; Raghavachari, K.; Pople, J. A. *J. Chem. Phys.* **1990**, *93*, 2537.
(37) Liu, Y.-P.; Lynch, G. C.; Truong, T. N.; Lu, D.-H.; Truhlar, D. G.; Garrett, B. C. *J. Am. Chem. Soc.* **1993**, *115*, 2408.
(38) Tucker, S. C.; Truhlar, D. G. In *New Theoretical Concepts for Understanding Organic Reactions*; Bertran, J.; Csizmadia, I. G., Eds.; Kluwer: Dordretch, The Netherlands, 1989; pp 291−346.
(39) Truong, T. N. *J. Chem. Phys.* **1994**, *11*, 8014.
(40) Truhlar, D. G.; Garrett, B. C. *J. Chem. Phys.* **1979**, *70*, 1593.
(41) Truhlar, D. G.; Garrett, B. C. *J. Chim. Phys.* **1987**, *84*, 365.
(42) Truhlar, D. G.; Garrett, B. C. *Annu. Rev. Phys. Chem.* **1984**, *35*, 159.
(43) Truhlar, D. G.; Isaacson, A. D.; Skodje, R. T.; Garrett, B. C. *J. Phys. Chem.* **1982**, *86*, 2252.
(44) Garrett, B. C.; Joseph, T.; Truong, T. N.; Truhlar, D. G. *Chem. Phys.* **1989**, *136*, 271.

used to calculate $P^G(E)$. When the reaction path curvature is negligible so that the tunneling path coincides with the MEP, the minimum energy path semiclassical adiabatic ground state (MEPSAG) method is appropriate.[45] If the reaction path is curved, tunneling is assumed to occur on the path defined by the classical turning points on the concave side of the MEP. This is called corner-cutting tunneling. When the curvature is small, the centrifugal-dominant small-curvature semiclassical adiabatic ground state (CD-SCSAG) tunneling approximation is appropriate.[37] When the reaction path curvature is large, which is typical for a bimolecular light-atom transfer between two heavy atoms, the large-curvature ground-state approximation, version 3 (LCG3), is appropriate.[31,44] In the LCG3 method, tunneling amplitudes are evaluated along all possible straight-line tunneling paths with equal kinetic energy before and after tunneling, and these tunneling amplitudes are weighted by the local speed and the vibrational period to give transmission probability. The contribution from tunneling along MEP is also included, but usually does not make a large contribution.

The MEPSAG, CD-SCSAG, and LCG3 methods are called "zero-curvature tunneling" (ZCT), "small-curvature tunneling" (SCT), and "large-curvature tunneling" (LCT), respectively. The detailed mathematical derivations and computational formulas have been discussed and reviewed elsewhere.[31,44−47]

Computational Method

All electronic structure calculations were done using the GAUSSIAN 92 and 94 quantum mechanical packages.[48,49] Geometries for formic acid, stable formic acid dimer complex, and the transition state were optimized at the Hartree−Fock (HF) level of theory using STO-3G, 6-31G, 6-31G(d,p), 6-31+G(d,p), 6-311G(d,p), and 6-311+G(d,p) basis sets and the second-order Møller−Plesset (MP) level of theory using the 6-31G(d,p) basis set. Energies at the stationary points have also been calculated at the G2* level theory.[34−36] Density functional theory calculations were also performed. Becke's three-parameter[50] gradient corrected exchange with the Lee−Yang−Parr[51] gradient corrected correlation (B3-LYP), using Dunning's double-ζ correlation consistent basis sets[52−54] with and without diffuse functions (aug-cc-pVDZ and cc-pVDZ), was used. In the standard G2 method, MP2/6-31G(d) is used for the optimization of the geometry and energy. In this study polarization functions on hydrogen were added because hydrogen bonding is important. So the G2 type of energies in this study will be called G2* energies. Using MP2/6-31G(d,p) geometries, single-point calculations were completed at the MP4/6-311G(2df,p), MP4/6-311+G(d,p), MP4/6-311G(d,p), MP2/6-311+G(3df,2p), and QCISD(T)/6-311G(d,p) levels. The MP4/6-311G(d,p) level was used as a starting point, and corrections were made for diffuse functions on non-hydrogen atoms, $\Delta E(+)$,

$$\Delta E(+) = \text{MP4/6-311+G(d,p)} - \text{MP4/6-311G(d,p)} \quad (4)$$

higher polarization functions on non-hydrogen atoms, $\Delta E(2df)$,

$$\Delta E(2df) = \text{MP4/6-311G(2df,p)} - \text{MP4/6-311G(d,p)} \quad (5)$$

with additional corrections for non-additivity, $\Delta E(+,2df)$,

$$\Delta E(+,2df) = [\text{MP2/6-311+G(2df,p)} - \text{MP2/6-311+G(d,p)}] - [\text{MP2/6-311G(2df,p)} - \text{MP2/6-311G(d,p)}] \quad (6)$$

basis set enhancement, $\Delta E(3df,2p)$,

$$\Delta E(3df,2p) = \text{MP2/6-311+G(3df,2p)} - \text{MP2/6-311+G(2df,p)} \quad (7)$$

correlation effects beyond fourth-order perturbation, $\Delta E(QCI)$,

$$\Delta E(QCI) = \text{QCISD(T)/6-311G(d,p)} - \text{MP4/6-311G(d,p)} \quad (8)$$

higher level correction, $\Delta E(HLC)$,

$$\Delta E(HLC) = -0.00019n_\alpha - 0.00481n_\beta \quad (9)$$

and the zero-point energy, ΔZPE.

The G2* energy includes all of these corrections:

$$E(G2^*) = \text{MP4/6-311G(d,p)} + \Delta E(+) + \Delta E(2df) + \Delta E(+,2df) + \Delta E(3df,2p) + \Delta E(QCI) + \Delta E(HLC) + \Delta ZPE \quad (10)$$

Diret dynamics calculations were performed using the MORATE program.[47] Frequencies were calculated as needed from MOPAC implemented in the MORATE[47] program, and the Page−McIver method[55] is employed to calculate the minimum energy path. To take the tunneling effect on the double proton transfer into account, the MEPSAG (ZCT), CD-SCSAG (SCT), and LCG3 (LCT) methods were used. In the LCG3 method, tunneling amplitudes are calculated only from the vibrational ground state of the reactant to the vibrational ground state of the product. Rates were calculated by canonical variational transition state theory using eqs 1−3 above.

Table 1. Dimerization Energies and the Barrier Height for the Double Proton Transfer

computational level	ΔE_d (kcal mol^{-1})[a]	ΔE^* (kcal mol^{-1})[b]
HF/STO-3G	−15.2	5.2
HF/6-31G	−19.1	15.6
HF/6-31G(d,p)	−15.2	16.6
HF/6-31+G(d,p)	−13.6	17.1
HF/6-311G(d,p)	−14.4	18.0
HF/6-311+G(d,p)	−12.9	18.4
MP2/6-31G(d,p)	−18.4 (−16.4)	8.0
ab initio MCPF[c]	−16.2 (−13.9)	9.3, 10.1
B3-LYP/cc-pVDZ	−20.8	5.2
B3-LYP/AUG-cc-pVDZ	−15.7	6.3
experimental	−14.4,[d] −14.8,[e] −14.1,[f] −11.7,[g] −12.0[h]	

[a] The numbers in parentheses are with zero-point energies. [b] The barrier height is the energy of the transition state minus that of FAD, neglecting zero-point energy. [c] Reference 30. [d] Reference 56. [e] Reference 57. [f] Reference 59. [g] Reference 58. [h] Reference 16.

Results and Discussion

The energies to form the formic acid dimer (FAD) from two formic acid monomers (FAM) and the barrier heights from the FAD complex to the double proton transfer transition state are listed in Table 1. The experimental enthalpies of formation for formic acid dimer are −86.67 and −187.7 kcal mol^{-1}, respectively.[56] From these two values the enthalpy of dimerization is 14.4 kcal mol^{-1} as listed in Table 1. Other experimental

(45) Garrett, B. C.; Truhlar, D. G.; Grev, R. S.; Magnuson, A. W. *J. Phys. Chem.* **1980**, *84*, 1730.
(46) Lu, D.-h.; Truong, T. N.; Melissas, V. S.; Lynch, G. C.; Liu, Y.-P.; Garrett, B. C.; Steckler, R.; Isaacson, A. D.; Rai, S. N.; Hancock, G. C.; Launderdale, J. G.; Joseph, T.; Truhlar, D. G. *Comput. Phys. Commun.* **1992**, *71*, 235.
(47) Hu, W.-P.; Lynch, G. C.; Liu, Y.-P.; Rossi, I.; Stewart, J. J. P.; Steckler, R.; Garrett, B. C.; Isaacson, A. D.; Lu, D.-h.; Melissas, V. S.; Truhlar, D. G. MORATE−Version 6.5, University of Minnesota, Minneapolis, 1995.
(48) Frisch, M. J.; Trucks, G. W.; Head-Gordon, M.; Gill, P. M. W.; Wong, M. W.; Foresman, J. B.; Johnson, B. G.; Schlegel, H. B.; Robb, M. A.; Replogle, E. S.; Gomperts, R.; Andres, J. L.; Raghavachari, K.; Binkley, J. S.; Gonzalez, C.; Martin, R. L.; Fox, D. J.; Defrees, D. J.; Baker, J.; Stewart, J. P.; Pople, J. A. Gaussian 92; Gaussian, Inc.: Pittsburgh, 1992.
(49) Frisch, M. J.; Trucks, G. W.; Schlegel, H. B.; Gill, P. M. W.; Johnson, B. G.; Robb, M. A.; Cheeseman, J. R.; Keith, T. A.; Petersson, G. A.; Montgomery, J. A.; Raghavachari, K.; Al-Laham, M. A.; Zakrzewski, V. G.; Ortiz, J. V.; Foresman, J. B.; Cioslowski, J.; Stefanov, B. B.; Nanayakkara, A.; Challacombe, M.; Peng, C. Y.; Ayala, P. Y.; Chen, W.; Wong, M. W.; Andres, J. L.; Replogle, E. S.; Gomperts, R.; Martin, R. L.; Fox, D. J.; Binkley, J. S.; Defrees, D. J.; Baker, J.; Stewart, J. P.; Head-Gordon, M.; Gonzalez, C.; Pople, J. A. Gaussian 94; Gaussian, Inc.: Pittsburgh, 1995.
(50) Becke, A. D. *J. Chem. Phys.* **1993**, *98*, 5648.
(51) Lee, C.; Yang, W.; Parr, R. G. *Phys. Rev. B* **1988**, 786.
(52) Dunning, T. H., Jr. *J. Chem. Phys.* **1989**, *90*, 1007.
(53) Woon, D. E.; Dunning, T. H., Jr. *J. Chem. Phys.* **1993**, *98*, 1358.
(54) Kendall, R. A.; Dunning, T. H., Jr.; Harrison, R. J. *J. Chem. Phys.* **1992**, *96*, 6796.
(55) Page, M.; McIver, J. W. *J. Chem. Phys.* **1988**, *88*, 922.
(56) Weast, R. C. *CRC Handbook of Chemistry and Physics*; CRC Press: West Palm Beach, 1979.

Table 2. G2* Energies of Formic Acid, Formic Acid Dimer, and Formic Acid Dimer Transition State[a]

	FAM	FAD	FADTS
MP2/6-311G(d,p)	−189.3515815	−378.7295361	−378.7157237
MP2/6-311+G(d,p)	−189.3620287	−378.7470777	−378.7331633
MP2/6-311G(2df,p)	−189.4473300	−378.9235341	−378.9132087
MP2/6-311+G(2df,p)	−189.4564184	−378.9381679	−378.9280097
MP2/6-311+G(3df,2p)	−189.4707282	−378.9674592	−378.9547629
MP4/6-311G(d,p)	−189.3838209	−378.7939062	−378.7789787
MP4/6-311+G(d,p)	−189.3947502	−378.8124120	−378.7974967
MP4/6-311G(2df,p)	−189.4844340	−378.9973048	−378.9856621
QCISD(T)/6-311G(d,p)	−189.3802017	−378.7867206	−378.7714457
$\Delta E(+)$	−0.0109293	−0.0185058	−0.018518
ΔE(2df)	−0.1006131	−0.2033986	−0.2066834
ΔE(+,2df)	0.0014218	0.0029078	0.0026386
ΔE(3df,2p)	−0.0143098	−0.0292913	−0.0257532
ΔE(QCI)	0.0036192	0.0071856	0.007533
ΔE(HLC)	−0.045	−0.090	−0.090
ZPE[b]	20.29617	42.52551	38.78609
E(G2*)	−189.5172881	−379.0572398	−379.0489521
rel energy[c]	0.0(0.0)	−14.22(−16.15)	−9.02(−7.21)

[a] Energies in hartrees. [b] In kcal mol^{-1}. Calculated from frequencies at the MP2/6-31G** level scaled by 0.9367. The zero-point energy of the imaginary frequency is set to zero for FADTS. [c] In kcal mol^{-1}. The energies of two monomers are set to zero. The numbers in parentheses are without zero-point energy. The barrier heights for the double proton transfer with and without zero-point energy are 5.20 and 8.94 kcal mol^{-1}, respectively.

dimerization energies are also listed.[16,57−59] The results in Table 1 show that the computed dimerization energy and the barrier height are very sensitive to the basis set and the treatment of the electron correlation effect.[33] In the density functional theory calculation, better agreement with experiment is obtained in the dimerization energy when the diffuse functions are included. These results do not provide energetic information about the double proton transfer that is accurate enough to be used as a protocol for the direct dynamics calculation. As accurate energetics as possible was needed to modify the standard AM1 parameters, so the G2* level of calculation was used. The results of the G2* calculation are listed in Table 2. The dimerization energy is −14.2 kcal mol^{-1}, which agrees very well with the experimental value. The basis set superposition error (BSSE) may be introduced when the basis set of the dimer is not consistent with that of the monomer.[11,25,60−65] The smaller basis set used for each monomer leads to a higher (less negative) energy via the variational principle, which leads to higher combined energy for the monomers.[25] This result produces larger energy difference between the monomers and the dimer (more negative dimerization energy) in general. In the G2 method, the BSSE is not corrected explicitly. However, the deficiency in the size of the basis set has been corrected individually for the monomer and the dimer in the standard G2 method as shown in eqs 4−7. The average deviation for the G2 energies from experimental atomization energies[66] of first-row compounds is known to be about 1 kcal mol^{-1}.[34−36] The error in the dimerization energy may be larger due to the BSSE, but further study is necessary to know how much the BSSE is involved in the G2 procedures. Generally the correction of the BSSE leads to less negative dimerization energy.[25] The

(57) Clague, A. D. H.; Bernstein, H. J. *Spectrochim. Acta* **1969**, *25*, 593.
(58) Henderson, G. *J. Chem. Educ.* **1987**, *64*, 88.
(59) Mathews, D. M.; Sheets, R. W. *J. Chem. Soc. A* **1969**, 2203.
(60) Boys, S. F.; Bernardi, F. *Mol. Phys.* **1970**, *19*, 553.
(61) Frisch, M.; DelBene, J. E.; Binkley, J. S.; Schaefer, H. F., III *J. Chem. Phys.* **1986**, *84*, 2279.
(62) Gutowski, M.; van Lenthe, J. H.; Verbeek, J.; van Duijneveldt, F. B. *Chem. Phys. Lett.* **1986**, *124*, 370.
(63) Latajka, Z.; Scheiner, S.; Chalasinski, G. *Chem. Phys. Lett.* **1992**, *196*, 384.
(64) Schwenke, D. W.; Truhlar, D. G. *J. Chem. Phys.* **1985**, *82*, 2418.
(65) Szczesniak, M. M.; Scheiner, S. *J. Chem. Phys.* **1986**, *84*, 6328.
(66) The experimental atomization energies have been obtained from the heats of formation given in the JANEF table.

Table 3. Specific Reaction Parameters

atom	parameter[a]	AM1	AM1-SRP
H	ζ_s	1.188078	1.050000
H	α	2.882324	2.982324
C	U_{pp}	−39.614239	−38.614239
C	ζ_s	1.8087	1.8387
C	ζ_p	1.685116	1.785116
O	β_s	−29.272773	−28.972773
O	β_p	−29.272773	−28.972773
O	ζ_s	3.108032	3.008032
O	G_{p2}	12.98	12.78

[a] ζ = Slater exponents; α = core−core repulsion integral; β = resonance integral; U_{pp} = one-center core-electron attraction, plus kinetic energy; G_{p2} = one-center electron repulsion integral.

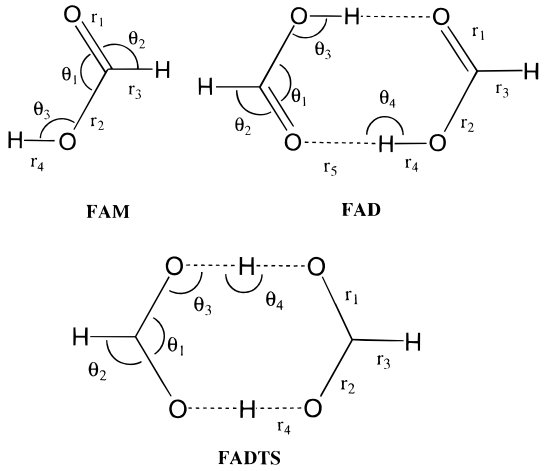

Figure 2. Geometries for formic acid monomer (FAM), formic acid dimer (FAD), and formic acid dimer transition state (FADTS).

Table 4. Theoretical and Experimental Geometries and Heat of Formation for the Formic Acid Monomer, Formic Acid Dimer, and the Transition State[a]

	expt	MP2/6-31G(d,p)	AM1	AM1-SRP
		FAM		
r_1	1.202	1.213	1.211	1.221
r_2	1.343	1.351	1.344	1.343
r_3	1.097	1.093	1.095	1.102
r_4	0.972	0.972	0.953	1.002
θ_1	124.6	125.1	117.5	115.8
θ_2	124.1	125.4	130.1	131.5
θ_3	106.3	106.1	110.5	113.2
ΔH_f	−86.67		−97.38	−86.40
		FAD		
r_1	1.217	1.230	1.234	1.230
r_2	1.320	1.320	1.349	1.327
r_3	1.079	1.092	1.104	1.104
r_4	1.033	0.995	0.976	1.020
r_5		1.711	2.101	1.855
θ_1	126.2	126.7	118.4	117.0
θ_2	115.4	122.0	128.9	128.9
θ_3	108.5	109.4	111.3	114.9
θ_4	(180.0)[b]	178.9	169.0	174.1
ΔH_f	−187.7		−201.2	−188.3
		FADTS		
r_1		1.269	1.286	1.274
r_2		1.269	1.286	1.274
r_3		1.091	1.107	1.105
r_4		1.204	1.200	1.214
θ_1		127.2	120.4	118.1
θ_2		116.4	119.8	121.0
θ_3		115.3	117.4	120.8
θ_4		177.8	175.2	179.6
ΔH_f			−164.3	−178.6
ΔE^* [c]		8.94(G2*)	36.9	9.64

[a] Distances in Å, angles in deg, and heats of formation in kcal mol^{-1}. [b] Assumed. [c] Barrier heights for the double proton transfer in kcal mol^{-1}.

dimerization energy of −14.2 kcal mol^{-1} at the G2* level agrees well within the experimental error limit. These energies were used to adjust the semiempirical MO parameters.

The NDDO level of semiempirical MO calculation of the enthalpies of formation with standard AM1 parameters gives −97.38 and −202.2 kcal mol^{-1} for formic acid and formic acid dimer, respectively, so the calculated enthalpy of dimerization is −7.4 kcal mol^{-1}. The calculated barrier height for the double proton transfer in the formic acid dimer with the G2* level of theory is 8.94 kcal mol^{-1}, but the barrier height from the semiempirical calculation using standard AM1 parameters is 36.9 kcal mol^{-1}. The standard AM1 parameters were adjusted, first, to reproduced the experimental structures and the enthalpies of formation for the FAM, and the FAD, and second, to reproduce the structure of the transition state and the barrier height from the G2* level of theory. The adjusted parameters are called specific reaction parameters (AM1-SRP).[32,37,67] Nine parameters were modified as listed in Table 3. Figure 2 shows the structural parameters. Table 4 gives both experimental and calculated values of these parameters, and the enthalpy of formation of FAM, FAD, and the transition state for the double proton transfer, denoted FADTS. The structures from the MP2/6-31G(d,p) level agree well with the experiments, and the AM1-SRP method reproduces the structures and the heats of formation for the FAM and FAD reasonably well. Both the AM1 and AM1-SRP methods give smaller values for θ_1 and larger values for θ_2 and θ_3 than the corresponding experimental values.[68−70] The AM1-SRP method reproduces the heat of formation very well. The dimerization energy and the barrier height for the double proton transfer from the AM1-SRP method are 15.5 and 9.64 kcal mol^{-1}, respectively. Table 5 shows the experimental and calculated frequencies for FAM, FAD, and FADTS. The MP2 frequencies were scaled by 0.9367, but the AM1 and AM1-SRP frequencies are not scaled. The HF values of frequencies are generally about 10% overestimated, so they are scaled by 0.9. Electron correlation reduces the error in HF values to about 5%.[71] The frequencies calculated at the MP2/6-31G(d,p) level were compared to the experimental frequencies for the FAM and the FAD.[14] The best agreement was obtained when the calculated frequencies are scaled by 0.9367. The scaled MP2 frequencies agree very well with the experimental values for the FAM and FAD.

The AM1 imaginary frequency for the double proton transfer TS is larger, but that from AM1-SRP is smaller than the imaginary frequency from the MP2/6-31G(d,p) calculation. In fact it is very difficult to get specific reaction parameters which reproduce the right structures, energies, and frequencies at the same time as pointed out previously.[39] The effect of a possible error in the imaginary frequency can be minimal if the most probable tunneling path is very different from the MEP as seen in most of the bimolecular heavy−light−heavy reaction dynamics systems.[30,31] Even though the standard AM1 parameters were adjusted based mainly on energies and structures, the frequencies for FAM and FAD from the AM1-SRP calculation show fairly good agreement with corresponding experimental frequencies. For FADTS, two frequencies with B_{1u} symmetry from AM1-SRP calculation are somewhat larger than those from the AM1 and MP2/6-31G(d,p) level calculations. These discrepancies were inevitable when the parameters were adjusted to reproduce the right energetics. To avoid these difficulties a direct *ab initio* dynamics approach has been suggested,[39,72,73] but the molecular system in this study is too large for this approach. All other frequencies maintain about the same level of accuracy as the standard AM1 level of semiempirical quantum mechanical calculation. The parameters listed in Table 3 were used for the direct dynamics calculation.

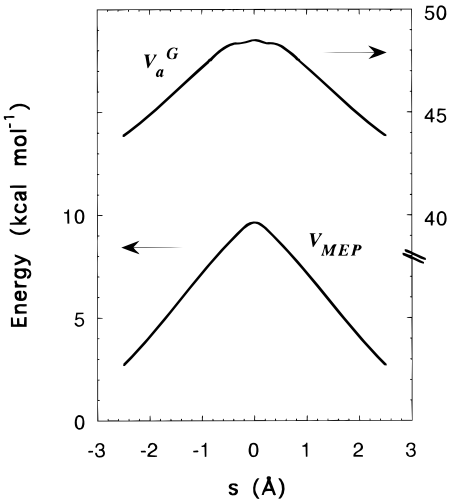

Figure 3. Born−Oppenheimer potential energy and the adiabatic ground state potential energy along the MEP.

Figure 3 shows the Born−Oppenheimer potential energy and the adiabatic ground state potential energy along the MEP for the double proton transfer. The adiabatic ground state potential energy, V_a^G, is the sum of the Born−Oppenheimer potential (V_{MEP}) and the local zero-point energy. The shape of the barrier is almost symmetric. Along the MEP the structure of the FAD maintains approximately C_{2h} symmetry, which indicates that the double proton transfer is a synchronous process.

The transmission coefficients and rate constants calculated using the ZCT and SCT approximations in the temperature range 200−400 K are listed in Table 6. The transmission coefficients using the ZCT approximation for the double proton transfer, κ_{HH}^{ZCT}, are smaller than that for the double deuterium transfer, κ_{DD}^{ZCT}, over the whole temperature range. The transmission coefficients using the SCT approximation show the same behavior. These results are the reverse of the general expectation that a light atom tunnels better;[74] however, the effect has been observed previously for low-barrier processes,[75,76] and its explanation lies in the fact[77] that the effective barrier for tunneling includes local zero-point energies so it is not the same for different isotopes. Nevertheless, the overall double proton transfer rate constants are still larger than the double deuterium transfer rate constants. The transmission coefficients, rate constants, KIE, the tunneling contribution to the KIE, and the quasiclassical KIE calculated using the LCT approximation in the temperature range 200−400 K are listed in Table 7. For the transmission coefficients using the LCT approximation in which nonadiabatic behavior is included[31,44,46] (so the local zero-point energy is not so important), κ_{HH}^{LCT} is larger than κ_{DD}^{LCT} at all temperatures. These results suggest that the ZCT and the SCT approximations do not represent the tunneling well for the

(67) Gonzalez-Lafont, A.; Truong, T. N.; Truhlar, D. G. *J. Phys. Chem.* **1991**, *95*, 4618.
(68) Almessingen, A.; Bastiansen, O.; Motzfeldt, T. *Acta Chem. Scand.* **1970**, *24*, 747.
(69) Almessingen, A.; Bastiansen, O.; Motzfeldt, T. *Acta Chem. Scand.* **1969**, *23*, 2848.
(70) Harmony, M. D.; Laurie, V. W.; Kuczkowski, R. L.; Schwendeman, R. H.; Ramsay, D. A.; Lovas, F. J.; Lafferty, W. J.; Maki, A. G. *J. Phys. Chem., Ref. Data* **1979**, *8*, 619.
(71) Bartlett, R. J.; Stanton, J. F. In *Reviews in Computational Chemistry*; Lipkowitz, K. B., Boyd, D. B., Eds.; VCH: New York, 1994; Vol. 5, p 65.
(72) Baldridge, K. K.; Gordon, M. S.; Steckler, R.; Truhlar, D. G. *J. Phys. Chem.* **1989**, *93*, 5107.
(73) Truhlar, D. G.; Gordon, M. S. *Science* **1990**, *249*, 491.
(74) Bell, R. P. *The Tunnel Effect in Chemistry*; Chapman and Hall: New York, 1980.
(75) Truong, T. N.; McCammon, J. A. *J. Am. Chem. Soc.* **1991**, *113*, 7504.
(76) Storer, J. W.; Houk, K. N. *J. Am. Chem. Soc.* **1993**, *115*, 10426.

Table 5. Experimental and Calculated Frequencies for FAM, FAD, and FADTS[a]

	FAM					FAD					FADTS		
	exp	MP2/6-31G**	AM1	AM1-SRP		exp	MP2/6-31G**	AM1	AM1-SRP		MP2/6-31G**	AM1	AM1-SRP
A′	3569	3565	3429	3253	Ag		3086	3377	3151	Ag	3001	3170	3143
	2942	2976	3191	3156		2949	2991	3185	3042		1612	1682	1699
	1777	1722	2050	2027		1670	1652	2028	1968		1334	1394	1272
	1381	1352	1491	1475		1415	1404	1504	1537		699	690	712
	1223	1248	1439	1306		1375	1349	1441	1291		490	461	445
	1104	1079	1232	1157		1214	1192	1240	1165	Au	81	81	72
	625	585	606	616		677	636	610	632	B1g	1274	829	817
A″	1033	1004	988	962		190	182	102	161	B1u	2999	3170	3143
	642	663	606	632		137	157	77	96		1361	1655	1817
					Bg	1060	1026	991	967		1266	1350	1649
							903	625	664		750	730	769
						230	255	161	228	B2g	1025	985	965
					Au	1050	1050	992	968		311	264	267
						917	925	651	716	B2u	1688	1952	1935
						163	167	60	102		1505	1382	1270
						68	67	43	46		1353	1247	1137
					Bu	3110	3180	3388	3152		555	523	522
						2957	2988	3185	3094	B3g	1702	2006	2011
						1754	1706	2047	2013		1354	1324	1270
						1450	1379	1506	1541		212	293	266
						1365	1336	1442	1285	B3u	1323	1013	978
						1218	1195	1242	1157		1014	806	856
						697	664	603	624		224	169	173
						248	243	193	287	B3g	−1261	−1797	−770

[a] In cm^{-1}. MP2/6-31G** frequencies are scaled by 0.9367.

Table 6. Transmission Coefficients and Rate Constants for Double Proton and Deuterium Transfer Calculated Using the ZCT and SCT methods

T(K)	$\kappa_{HH}^{1.29}$	κ_{DD}^{ZCT}	k_{HH}^{ZCT}	k_{DD}^{ZCT}	κ_{HH}^{SCT}	κ_{DD}^{SCT}	k_{HH}^{SCT}	k_{DD}^{SCT}
200	1.29	1.50	3.38×10^5	1.39×10^4	2.56	3.16	6.70×10^5	2.93×10^4
250	1.17	1.29	5.15×10^6	3.79×10^5	1.82	2.07	8.03×10^6	6.10×10^5
300	1.12	1.19	3.20×10^7	3.46×10^6	1.51	1.66	4.34×10^7	4.82×10^6
350	1.08	1.14	1.17×10^8	1.70×10^7	1.36	1.45	1.47×10^8	2.16×10^7
400	1.06	1.10	3.12×10^9	5.60×10^7	1.26	1.33	3.71×10^8	6.77×10^7

Table 7. Transmission Coefficients, Rate Constants for Double Proton and Deuterium Transfer, Kinetic Isotope Effects, and Tunneling Contribution to the Kinetic Isotope Effect Calculated Using the LCT Method

T (K)	κ_{HH}^{LCT}	κ_{DD}^{LCT}	k_{HH}^{LCT}	k_{DD}^{LCT}	KIE^{LCT}	$\kappa_{HH}^{LCT}/\kappa_{DD}^{LCT}$	KIE_{qc}
200	155	31.6	4.06×10^7	2.94×10^5	139	4.91	28.3
250	47.6	10.6	2.10×10^8	3.11×10^6	67.6	4.50	15.0
300	21.9	5.44	6.28×10^8	1.58×10^7	39.7	4.03	9.85
350	12.7	3.54	1.37×10^9	5.28×10^7	26.0	3.58	7.26
400	8.45	2.65	2.48×10^9	1.35×10^8	18.3	3.19	5.74

double proton transfer in the FAD complex, but the LCT approximation does.

In fact the reaction path curvature in the double proton transfer is fairly large. The angle between the MEP and a linear tunneling path from a pre-tunneling configuration at $s = -a$ to a post-tunneling configuration at $s = a$ are shown in Figure 4 for the double proton transfer and the deuterium transfer. At the transition state ($s = 0$), the angle is zero. As the reaction goes toward either reactant ($s = -\infty$) or product ($s = +\infty$) the angle increases very rapidly. This indicates that the reaction path curvature is very large near the transition state. The angles at the representative tunneling path (the path which has maximum thermally weighted transmission probability[77]) are 73° at $s = 1.33$ and 64° at $s = 1.13$ for the double proton transfer and the double deuterium transfer, respectively. These are also shown in Figure 4. The representative tunneling path (RTP) of the double proton transfer is further from the transition state than that of the double deuterium transfer, which is reasonable since the less massive particle has higher probabilities to tunnel.

Figure 5 shows the transmission probabilities calculated by the ZCT, SCT, and LCT approximations, and the thermally

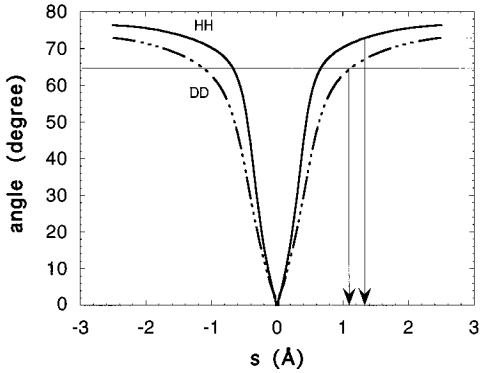

Figure 4. Angles between the gradient on the MEP and the large curvature tunneling path along the reaction coordinate. The two horizontal lines represent the angles at the representative tunneling path for double proton transfer at $s = 1.33$ and for double deuterium transfer at $s = 1.13$.

weighted transmission probabilities from the LCT method as a function of V_a^G for the double proton transfer. The LCT transmission probabilities are much larger than ZCT and SCT probabilities at all energies. The ZCT and SCT probabilities

(77) Truhlar, D. G.; Kuppermann, A. *J. Am. Chem. Soc.* **1971**, *93*, 1840.

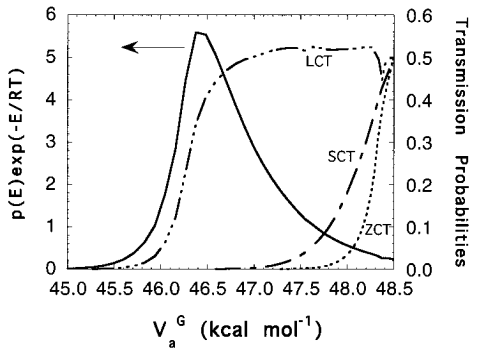

Figure 5. Transmission probabilities for double proton transfer from the ZCT, SCT, and LCT approximations and the thermally weighted transmission coefficient (solid line, scaled by 10^{-35}) from the LCT approximation as a function of the adiabatic ground state potential energy, V_a^G.

Figure 6. The pre-tunneling and post-tunneling configurations at the representative tunneling path. The values of r_1 and r_2 at the pre-tunneling configuration are 1.042 and 1.471 Å, respectively. The values of r_1 and r_2 are reversed at the post-tunneling configuration.

fall off very rapidly when a V_a^G is decreased, while the LCT probability remains near 0.5 until the energy is lowered by about 2 kcal mol^{-1}. This indicates that large curvature tunneling is an important element in the double proton transfer of the FAD complex. From the thermally weighted transmission probabilities, the RTP was estimated. This occurs when V_a^G is 46.42 kcal mol^{-1}. This is about 2 kcal mol^{-1} below the top of the minimum adiabatic energy barrier. The potential energy at the RTP is 6.16 kcal mol^{-1} which is about 3.5 kcal mol^{-1} below the top of the minimum potential energy barrier. The potential energy surfaces for single hydride transfer between NAD^+ analogues in solution has been studied and the RTP occurs about 1 kcal mol^{-1} below the top of the potential energy barrier.[78] For the hydride transfer reactions, experimental kinetic isotope effects were available, and the analytical potential energy functions were fitted to reproduce them. Since the isotope effects are very sensitive to the transmission probabilities it is unlikely that the RTP was badly misplaced. These results suggest that tunneling for the double proton transfer in the FAD complex is very efficient, and the RTP is very different from the MEP, as also suggested by Shida *et al.*[30] It is concluded that the imaginary frequency at the transition state is not a crucial parameter for the dynamics of the double proton transfer in the FAD complex because most reactive paths do not pass close to the transition state.

Figure 6 shows the pre-tunneling configuration and the post-tunneling configuration for the RTP. These two structures are symmetric and belong to the C_{2h} point group. The distances r_1 and r_2 at the pre-tunneling configuration are 1.042 and 1.471 Å, respectively. The actual distance that the proton hops by tunneling is 0.429 Å. This distance is considerably larger than the same distance for the hydride transfer between NAD^+ analogues which is about 0.1 Å.[78] The distances r_1 and r_2 in the most stable FAD complex are 1.020 and 1.855 Å, respectively. In converting the most stable FAD to the configuration of the RTP the nonbonded O−O distance is reduced by 0.362 Å, while the bonding O−H distance is increased by only 0.022 Å. Thus it is mostly heavy atoms that move when the reaction goes from the FAD complex up to the pre-tunneling configuration, and suddenly the two protons hop at that point. These results are the same as those of Shida *et al.*[30]

The calculated kinetic isotope effects (KIE) at the various temperatures are also listed in Table 7. The KIE calculated using the LCT approximation at 300 K is very large, especially when one considers that the KIE in single proton transfers are usually in the range of 5−10, rising to about 20 in a few cases near room temperature.[2,74] Limbach *et al*. have determined the KIEs in other synchronous double proton transfers using dynamic NMR method.[6,7] The KIE in the double proton transfer between acetic acid and methanol is 15 at 298 K,[7] and that in the substituted formamidine dimer is 237 at 189 K.[6] The former is smaller, but the latter is larger than the KIE calculated using the LCT method. The tunneling contribution to the KIE, $\kappa_{HH}^{LCT}/\kappa_{DD}^{LCT}$, is not very large compared with the total KIE. This is not because the tunneling effect is small, but because the values of both κ_{HH}^{LCT} and κ_{DD}^{LCT} are fairly large compared with the corresponding single proton transfer values. The reaction path curvature for the double deuterium transfer is also fairly large, so the values of κ_{DD}^{LCT} are larger than the corresponding single deuterium transfer values. The large KIE is mainly due to a large quasiclassical contribution, KIE_{qc}. This is due to the synchronous hydrogenic motion of the two protons in flight, which raises the zero-point energy contribution to the KIE. If we assume the rule of the geometric mean, the quasiclassical contribution from each proton becomes 3.14 at 300 K, which is very reasonable.[2,74,78] The values of KIE_{qc} vary considerably with temperature. KIE_{qc} includes contributions from the rotational and translational partition functions, in addition to those from the vibrational partition functions. The rotational and translational partition functions do not vary much with temperature, so the change in KIE_{qc} is mainly due to the change in the vibrational partition functions. This suggests that the KIE in the double proton transfer has a fairly large entropic contribution. This will be discussed in a future study.

Concluding Remarks

The double proton transfer reaction of the FAD complex has been studied with canonical variational transition state theory using multidimensional semiclassical tunneling approximations. The MEP was calculated by a direct dynamics approach using the AM1-SRP method. The barrier height for the double proton transfer has been calculated with high-level *ab initio* calculations. From calculations at the G2* level the barrier height is estimated to be 8.94 kcal mol^{-1}.

The reaction path curvature is large, so large curvature tunneling is very efficient. The representative tunneling path (RTP) occurs about 3.5 kcal mol^{-1} below the top of the potential energy barrier and is very different from the MEP. The distance that two protons hop is 0.429 Å, which is very large. The kinetic isotope effect is also very large. The quasiclassical contribution to the KIE is considerably larger than that observed for single proton transfer. This is due to the synchronous hydrogenic motion of the two protons in flight. Further study is necessary to understand the KIE better.

Acknowledgment. The author thanks Professors Maurice M. Kreevoy and Donald G. Truhlar for helpful comments. This work has been supported by a grant from Kyung Hee University.

JA953175V

(78) Kim, Y.; Truhlar, D. G.; Kreevoy, M. M. *J. Am. Chem. Soc.* **1991**, *113*, 7837.